Study of Impact of Forecasting Methods on Reliability of Renewable Energy sources

Sumbul Hasan
EED, IIT Bomaby, Mumbai 40076
Email:sumbulHasan@ee.iitb.ac.in

Himanshu J Bahirat
EED, IIT Bomaby, Mumbai 40076
Email:hjbahirat@ee.iitb.ac.in

***Abstract*—Wind power plants (WPP) are intermittent source of energy unlike conventional power plants, it is difficult to firmly dispatches them. Modern grid codes requires the wind power plants to be dispatched like traditional power plants, for this reason wind farm operator have to rely on prediction for short term wind power to schedule wind farm. Wind farm operators submit the bids in day ahead market based on forecasted wind power while updated wind forecast is used for hedging the bids in the electrical market. Any deviation of the actual wind power generation from the schedule wind generation is either adjusted by purchasing /selling energy in real time market, otherwise wind farm operators have to pay deviation cost as penalty. Hereby, the accuracy of the prediction system has economical and technical impact on the operation of grid with high RES penetration. In this proposed paper, comparison of three well known prediction methods like Persistence, ARIMA, Markov chain is made by evaluating the statistical metrics like mean absolute error (MAE) and root mean square error (RMSE). A well-established operating strategy min-max method is used to control the operation of the BESS connected to the wind farm. The impact of accuracy of the different method of wind forecasting on the reliability of the system is studied in this paper by evaluating reliability indices like energy served (ES), energy not served (ENS) and energy not utilised (ENU).**

I. Introduction

The stochastic nature of wind power makes it difficult to operate WPP like conventional power plant. Large scale grid integration of the RES has a great impact on real time grid operation, ancillary service requirement, power quality, upgradation of transmission network, competitive market design, reliability and security of the grid, reduction of green house gases and other environmental benefits [1], [2]. An accurate wind prediction is required over a wide range from seconds to days to be used for primary frequency regulation, reactive power support, power oscillation damping service [3].

From the literature it is seen that wind speed forecasting can be (1) weather-based (2) time-series-based [4]. The weather based method uses hydrodynamic atmospheric model which assimilates physical phenomena like frictional, thermal and conventional effects [5], [6]. The time series based prediction method uses data available from site to build the statistical model to be used for forecasting [7]–[9]. There are several time series based methods to predict wind speeds for example: Persistence, ARIMA and Markov chain methods [8], [10], [11]. These are methods are usually compared with respect to performance by evaluating statistical metrics like root mean square error, mean absolute error [12], [13] . The literature survey indicates for short term wind forecast second order Markov model is more accurate than Persistence and ARMA models [12]. It is observed from literature survey various methods and their comparison has been made but the impact of the different forecasting model on the reliability of the wind farm in meeting the schedule dispatches has not been studied. Through this paper we want to address the gaps identified in the literature survey and hereby study the impact of accuracy of the wind forecast on the BESS size and the reliability of wind farm.

The operating strategy, also referred to as control strategy, of the storage, is usually defined to manage the BESS energy and lifetime. BESS is also used as energy buffer to mitigate the intermittent behaviour of RES and also to meet the schedule dispatches of RES. The minute-by-minute, model predictive control (MPC), min-max, pre-compensation, post compensation method as discussed in [14]–[17].

The minute-by-minute BESS operating strategy is used to benchmark performance of other operating strategies [14], [15]. In this strategy, BESS does not operates when the error between the forecast wind power and actual wind power is less than 2% and when error exceed 2%, BESS discharges or charges to reduce the error. The statistic like RMSE and MAE obtained for minute-by-minute method are better than moving horizon predictive control method as reported in [14]. The size of the storage obtained for pre-compensation method and post-compensation method is smaller than for minute-by-minute method [15]. The operating strategy presented in [14], [15], authors have reported BESS life reduction due to incomplete charging and discharging cycles.

The objective of the paper is to compare various forecasting methods with respect to their impact on the reliability indices. Thus, based on the literature survey, persistence, ARIMA and Markov chain methods are identified as candidate methods for evaluation. The dependence of reliability indices on the operating strategy is important and thus, min-max method is selected to ensure maximum BESS lifetimes. The outline of the paper is as follows: different forecasting methods are briefly summarized in Section II, the accuracy of the forecasting model is determined by finding forecasting errors as discussed in Section III, the operating strategy is presented in Section IV, system description is presented in Section V and obtained results are presented in Section VI. Finally, major conclusions are presented in Section VII.

II. Wind Forecasting Methods

A. Persistence Method

The persistence method is a classical method which is used as a benchmark for performance evaluation of forecasting methods. The method assumes a quasi-stationary model of the atmosphere [18], hence, the wind speed in the next interval is predicted to be equal to the measured value in the present interval as given by (1). Due to this the method is also termed as the naive method. The persistence method is known to have good accuracy for very short intervals of prediction i.e. ranging from few seconds to 30 minutes ahead and also for short intervals ranging from 30 minutes to 6 hours ahead [1].

$$\hat{V}(t+1|t) = V_t \tag{1}$$

B. ARIMA Method

The autoregressive integrated moving average (ARIMA) model is a class of stochastic processes used for time series analysis and forecasting [19]. ARIMA (p,d,q) model has three parameters, where p gives the order of the autoregressive(AR) part, d gives number of times first differencing involved to make time series stationary and q gives the order of the moving average(MA) part. The stationarity of time series is established by considering the ACF and PACF plots. If the ACF is exponentially decaying and PACF is significant till p lags for the stationary time series, then it is ARIMA(p,0,0) or AR(p) as model as given by (2). If ACF is significant till p lags and PACF decays with the increase in lag, then it is a ARIMA(0,0,q) or MA(q) model given by (3). For mixed ARIMA(p,0,q) or ARMA(p,q) model given by (4) both ACF and PACF decays with the increase in lag.

$$\hat{V}_t = \Phi_1 V_{t-1} + \cdots + \Phi_p V_{t-p} + \epsilon_t \tag{2}$$

where $V_{t-1}, V_{t-2}, \ldots V_{t-p}$ in (2) are wind speed in previous intervals and $\Phi_1, \Phi_2, \ldots \Phi_p$ are AR parameters which can be obtain from Yule-Walker equation [19].

$$\hat{V}_t = \epsilon_t - \theta_1 \epsilon_{t-1} - \cdots - \theta_q \epsilon_{t-q} \tag{3}$$

In (3), $\epsilon_t, \epsilon_{t-1}, \ldots \epsilon_{t-q}$ are independent and identically distributed (iid) white noise.

$$\hat{V}_t = \Phi_1 V_{t-2} + \cdots + \Phi_p V_{t-p} + \epsilon_t - \theta_1 \epsilon_{t-1} - \cdots - \theta_q \epsilon_{t-q} \tag{4}$$

The MA parameters $\theta_1, \theta_2, \ldots \theta_q$ in (3) and (4) are obtained using the invertibility condition [19].

In order to forecast the wind speeds based on AR(p) model Weiner-Kolomogrov prediction formula is used and is given by (5). The formula requires the mean wind speed value in addition to the AR parameters.

$$\begin{aligned}\hat{V}(t+k|t) &= \mu + \Phi_1(V(t)-\mu) + \Phi_2(V(t-1)-\mu) \\ &+ \ldots. + \Phi_p(V(t-p+1)-\mu)\end{aligned} \tag{5}$$

C. Markov Chain Method

Another method used in the study of stochastic processes is the Markov Chain Method [8], [20]–[22]. This method relies on enumerating states that a variable or system can take and defines probability of transition from one state to another [8]. The transition probabilities may be calculated or estimated empirically [8], [20]–[22]. Since it is possible to segregate the wind speed values into definite number of states and probabilities of transition from one state to other can be estimated, Markov Chain method has been used for generation and forecasting wind speeds [8], [20]–[22].

In order to establish the Markov Chain model for wind speeds, the wind speed time series is divided into different states. These states are given as $\mu \pm \sigma$, μ, $\mu \pm 2\sigma$, $\mu + \pm 3\sigma$ where μ is mean wind speed and σ is standard deviation of the wind speed. These values are obtained from the measured wind speed data. It is well reported in [8], higher discretization leads to better representation of the process but introduces a large number of parameters that are difficult to assess from the data .

The Markov Chain Method requires probability of transition from one state to the other. This is defined as a conditional probability of transitioning to a new state given the probability of being in the present state. For this purpose, if we consider X_t to be a stochastic process, having $i = 1, 2, 3 \ldots k$ discrete states, corresponding to a sequence of events at time instances $t_1 < t_2 < t_3 \cdots < t_k$. The conditional probability p of the process X_{tn} being in i_n^{th} state at time t_n can be given by (6). The probability is seen to depend on the history of the states the process follows [8], [20]–[22].

$$p = P_r \left\{ X_{tn} = i_n | X_{t1} = i_1, X_{t2} = i_2, ..., X_{tn-1} = i_{n-1} \right\} \tag{6}$$

1) First order Markov chain(FOM): If, the conditional probability of transition in a Markov process depends only on the present state and no other past states, then the process is termed as FOM. This is given by the (7) where probability of transitioning to $(i+1)^{th}$ state only depends on the i^{th} state [8], [20]–[22]. For a n state process, the conditional probabilities for transition can be represented in matrix form given by (8). The elements of the matrix represent probability of transition from i^{th} to j^{th} state at any instant of time [8], [20]–[22]. According to the FOM the probability of the stochastic process X_{tn} at instant t_n to be in state i_n if it was in state i_{n-1} in the previous state as given in (7). It seen from (7), state of the process does not depend on the process history but only depends on the previous state of the system.

$$p = P_r \left\{ X_{tn} = i_n | X_{tn-1} = i_{n-1} \right\} \tag{7}$$

$$P = \begin{bmatrix} p11 & p12 & .. & .. & p1n \\ p21 & p22 & .. & .. & p2n \\ : & : & : & : & : \\ : & : & : & : & : \\ pn1 & pn2 & .. & .. & pnn \end{bmatrix} \tag{8}$$

In the context of wind speed forecasting, the transition probabilities can be obtained using maximum likelihood method as given by (9) [8], [20]. The value of n_{ij} is equal to number of transitions taking place from ith to jth state.

$$p_{ij} = \frac{n_{ij}}{\sum_j n_{ij}} \ \forall i, j \ ; \ \sum_j p_{ij} = 1 \ \forall i \tag{9}$$

2) Second order Markov (SOM): Higher order Markov chains are created to have multiple time step memory [23]. Higher order Markov chain can very efficiently predict wind speed using additional memory they have regarding the wind data, which can be regarded as if features of the training models have been enhanced. Like SOM and higher order Markov chain uses more than one previous state in modelling the Markov chain. In a SOM process, the probability of the process to be in state i^{th} at time t depends on system states at t_1 and t_2 time instants, as given by (10) [8]. Based on the Chapman-Kolomogrov equation, the transition matrix for SOM can be easily obtain by squaring the FOM transition matrix [8], [24]. The second order model allows to improve the forecast performance by reducing the prediction error as reported in [8], [20]

$$p = P_r \left\{ X_{tn} \right) = i_n | X_{tn-1} = i_{n-1}, X_{tn-2} = i_{n-2} \right\} \tag{10}$$

The wind speed may be forecasted either by using FOM or SOM. The cumulative transition matrix for this is obtained from transition matrix (8). To forecast the wind speed a initial state is randomly chosen, then a uniform random number lying between zero and one is generated. The next state is found when the random number is greater than cumulative value of previous state and less than equal to cumulative value of next state. The wind predicted speed state has to be converted back into actual wind speed using the relationship given in (11) [20].

$$V = V_l + Z_i(V_l - V_u) \tag{11}$$

In (11), V_l and V_u are the lower and upper boundary of the state and Z_i is the uniform random number lying between zero and one [20].

III. Forecasting Error

The prediction models discussed in Section II are implemented and used on the measured wind speed data. The developed wind speed forecasting models are checked for correctness and their performance. For this purpose, the available data is divided into training and testing data. The training data is used to determine the model of each of the forecasting method. The predicted data is then compared with the measured data to determine the performance of the prediction method. In order to evaluate performance, the factors like prediction error, mean absolute error (MAE) and root mean square error (RMSE) are calculated.

A. Prediction error

Prediction error are obtained as a difference between the measured and predicted value at time $t + k$ as given in (12), where $V(t + k)$ is actual wind speed at time $t + k$ and $\hat{V}(t + k|t)$ is wind speed predicted at time t for instant $t + k$. This results in generation of time series of errors which is used for determination of MAE and RMSE.

$$e(t + k|t) = V(t + k) - \hat{V}(t + k|t) \tag{12}$$

1) Mean absolute error : The MAE, also known as the first moment, is calculated from the prediction error time series obtained from (12) by using (13) and it represents the average error of the forecasting model.

$$\text{MAE} = \frac{1}{N} \sum_{t=1}^{N} |e(t + k|t)| \tag{13}$$

2) Root mean square error: The RMSE, also known as the second moment, is calculated from the prediction error time series by using (14) and (15). Since, it is the second moment, the RMSE depends on the variance of the prediction error.

$$\text{MSE} = \frac{1}{N} \sum_{t=1}^{N} \left(e^2 \left(t + k|t \right) \right) \tag{14}$$

$$\text{RMSE} = \sqrt{\text{MSE}} \tag{15}$$

It may be observed that unlike MAE, RMSE is the weighted average of the error and gives more weightage to large errors. Hence if there is large difference between the predicted and the actual wind speed RMSE is expected to be larger than MAE.

IV. Operating Method

A. Power and Energy Rating of BESS

Generally, the size of a battery energy storage (BESS) is done to overcome the highest power deficit. The power deficit of a wind farm at any time t can be given by (16). The power P_{sch} gives the value of schedule wind power based on the forecasting methods, whereas P_w represents measured power being produced by the wind farm at time t. Thus the error in the schedule and prediction wind power has to be overcome by BESS.

$$P_{Sch}^{error}(t) = P_{sch}(t) - P_w(t) \tag{16}$$

The capacity of the BESS capacity, usually given by energy and power rating, should be adequate to overcome the largest prediction error given by (17). The energy rating of the BESS needs to consider the duration for which it is to be operated. In this paper duration is assumed to be one hour leading to ratio of energy to power capacity being equal to one.

$$P_{rating} = max[|P_{Sch}^{error}|] \tag{17}$$

B. Operating Method

The operating strategy plays a significant role in the BESS life management and is also expected to impact the reliability characteristics. With this view point, the min-max operating strategy is adopted in the paper. The min-max strategy uses short term wind power forecast time series to determine the dispatch power value. When the BESS is discharging, dispatched power is the maximum value of wind power in that dispatched interval. While when BESS is charging, dispatch power is minimum wind power of that dispatch interval.

Since, the operating method depends on accuracy of forecast and the accuracy of the forecast depends on the time horizon of the forecast. Shorter the prediction horizon more accurate would be forecast as reported in [25]. Error between the actual wind speed and the forecasted wind speed can be quantified in terms statistical parameters such as mean of wind speed error μ_v and the standard deviation σ_v of wind speed error. Thus, the maximum, central and minimum forecast values are obtained with 99.7% confidence intervals. This implies three standard deviations from the mean being considered for definition of maximum, minimum and central forecast values.

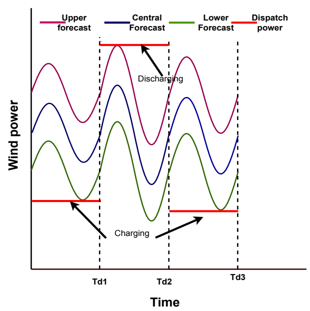

Fig. 1: Dispatched power for min-max operating strategy

The three standard deviations from the mean being considered for definition of maximum, minimum and central forecast values can be obtain as $\hat{V}(t)+\mu_v+3\sigma_v$, $\hat{V}(t)+\mu_v$ and$\hat{V}(t)+\mu_v-3\sigma_v$ respectively [16], [17]. Wind power corresponding to upper, central and lower wind power forecast range P_w^u, P_w^c and P_w^l respectively can either be calculated using speed-power characteristic of wind turbine and using $\hat{V}(t)+\mu_v+3\sigma_v$, $\hat{V}(t)+\mu_v$ and$\hat{V}(t)+\mu_v-3\sigma_v$ respectively or are determined as $\hat{P_{Sch}}(t)+\mu_P+3\sigma_P$, $\hat{P_{Sch}}(t)+\mu_P$ and$\hat{P_{Sch}}(t)+\mu_P-3\sigma_P$ respectively, where μ_P and σ_P are mean and standard deviation of schedule power error. While determining lower wind power forecast, if it assumes negative value as a result of statistical calculation, these negative value should be set to zero. Similarly if upper wind forecasted power takes value greater than wind turbine installed rating should, its value should be set to wind turbine installed rating.

To implement min-max operating strategy considering the given forecast wind power confidence interval, when BESS is discharging, P_d is fixed at the maximum value of P_w^u during dispatch interval and when BESS is charging P_d is fixed at minimum value of P_w^l during dispatch interval as shown in Fig. 1. Thus, the confidence interval effects the BESS operation and if confidence interval is increased it leads to frequent BESS operation and eventual reduction in the lifetime of BESS.

C. Operating Constraints

In order to determine charging and discharging of the BESS theP_w^u, P_w^c and P_w^l are used. For a BESS, state of charge (SOC) constraints SOC^{min} and SOC^{max} are specified to 0.2 and 0.9 respectively. The power exchanged by the BESS depends on the SOC constraints as given by (19). In (19) Δt is dispatched interval, η is round trip efficiency of BESS taken as 80% and E_r rated energy capacity of BESS.

$$Pb_t = P_w^c - P_d(t) \tag{18}$$

$$Pb(t) = \begin{cases} P(t), & SOC(t+1) \geq SOC^{min} \\ \frac{SOC^{min}-SOC(t)}{\eta \Delta t E_r}, & SOC(t+1) < S^{min} \\ P(t), & SOC(t+1) \leq SOC^{max} \\ \frac{SOC^{max}-SOC(t)}{\eta \Delta t E_r}, & SOC(t+1) > SOC^{max} \\ -Pb^{rated}, & Pb(t) < -P_b^{rated}; SOC(t) \neq SOC^{min} \\ Pb^{rated}, & Pb(t) > P_b^{rated}; SOC(t) \neq SOC^{max} \end{cases} \tag{19}$$

In (19), first and third constraint describes power delivered by BESS to grid when state of charge constrain are not violated. Second and fourth constraints gives the power delivered by BESS when state of charge constraint are violated. Fifth and sixth constraints in (19) describes the input or output of BESS can not exceed the power rating P_b^{rated} of converter. The state of charge of BESS at the start of the next interval depends on the state of charge at the beginning of the previous interval and the power supplied/sinked by BESS during the previous interval as given in (20).

$$\text{SOC(t+1)} = \text{SOC(t)} + \frac{\eta P_b(t)\Delta t}{E_r} \tag{20}$$

D. Reliability indices

In order to determine the effect of the wind forecast accuracy, reliability indices energy served (ES), energy not served (ENS) and energy not utilised (ENU) for each dispatched interval is calculated. The ES is equal to energy supplied by the wind farm and BESS in a dispatch interval when BESS is discharging and when the BESS is charging energy served is equal to dispatched energy as given in (21).

$$\text{ES(t)} = \begin{cases} (P_w^c(t) - Pb(t))\Delta t, & Discharging \\ P_d(t)\Delta t, & Charging \end{cases} \tag{21}$$

$$\text{ENS(t)} = \begin{cases} P_d(t)\Delta t - ES(t), & Discharging \\ 0, & Charging \end{cases} \tag{22}$$

The ENS in a dispatched interval can be obtain from (22), when the BESS is discharging ENS during a dispatch interval is difference of energy dispatched and energy served otherwise it is zero. The ENU given by (23), when BESS is discharging ENU is zero otherwise it is equal to difference of wind energy generated and energy dispatched and supplied by BESS.

$$\text{ENU(t)} = \begin{cases} 0, & Discharging \\ (P_w^c(t) - P_d(t) - Pb(t)\Delta t, & Charging \end{cases} \tag{23}$$

The expected energy served (EES), expected energy not served (EENS) and expected energy not utilised (EENU) can be obtain from (21), (22) and (23) by taking mean of ES, ENS and ENU over simulation horizon respectively.

V. System Description

The aggregated model of the wind farm is considered, where 150 wind turbines of 2 MW rating are represented by equivalent wind turbine with the rated power output P_r of 300 MW. The wind farm in feed wind energy into the grid. A centralized storage is connected at the point of common coupling through voltage source converter to absorb the wind variability.

In this paper we have consider three test case:-in first case we have used persistence method to make day ahead wind forecast, min-max method is used to manage BESS, the performance of the forecast method is evaluated by obtaining reliability indices . In the second and third test case we have used SOM and AR(2) for making day ahead wind forecast and again the reliability indices are evaluated when min-max method is used for operating BESS.

VI. Results

A. Wind Forecast

1) Persistence Model: The actual wind speed is time series data recorded at a site has been used for forecasting. From Fig. 3a it is observed the wind speed forecasted using persistence model plot is similar to the actual wind speed.

2) Markov Model: The Markov model for wind forecast has been discussed in detail in section II-C. The wind speed time series is divided into six classes and the probability of transition from one class to the other class is used to obtain transition probability matrix p as given by (24).

$$P = \begin{bmatrix} 0.8669 & 0.1269 & 0.0050 & 0.0012 \\ 0.0584 & 0.8510 & 0.0828 & 0.0078 \\ 0.0023 & 0.1874 & 0.6511 & 0.1593 \\ 0 & 0.0070 & 0.1441 & 0.8489 \end{bmatrix} \quad (24)$$

The cumulative transition matrix is obtain from (24) by performing cumulative summing within each row. In cumulative transition matrix each row end with one as given by (25).

$$P_{cum} = \begin{bmatrix} 0.8669 & 0.9938 & 0.9988 & 1 \\ 0.0584 & 0.9094 & 0.9922 & 1 \\ 0.0023 & 0.1897 & 0.8407 & 1 \\ 0 & 0.0070 & 0.1511 & 1 \end{bmatrix} \quad (25)$$

As we have discussed in section II-C2 that higher order Markov chain are more efficient in predicting wind speed accurately so we have develop SOM model for the wind speed prediction. The transition matrix for SOM model is obtained using Chapman- Kolmogorov equation as (26) from (24).

$$P^2 = \begin{bmatrix} 0.7590 & 0.2189 & 0.0182 & 0.0039 \\ 0.1005 & 0.7472 & 0.1258 & 0.0265 \\ 0.0145 & 0.2828 & 0.4624 & 0.2403 \\ 0.0007 & 0.0388 & 0.2168 & 0.7437 \end{bmatrix} \quad (26)$$

Cumulative transition matrix for SOM is given as (27).

$$P_{cum} = \begin{bmatrix} 0.7590 & 0.9778 & 0.9961 & 1 \\ 0.0584 & 0.8477 & 0.9735 & 1 \\ 0.0145 & 0.2973 & 0.7597 & 1 \\ 0.0007 & 0.0396 & 0.2563 & 1 \end{bmatrix} \quad (27)$$

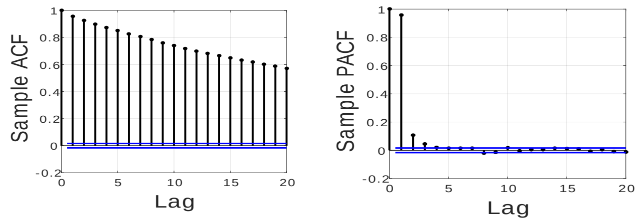

(a) Autocorrelation function (b) Partial Autcorrelation function

Fig. 2: ACF and PACF

Wind speed forecasting based on FOM and SOM can be obtain using (25), (27) and (11). Since the wind speed forecasting is done by predicting the next state of the wind speed randomly hence every time algorithm is run, forecasted wind speeds are different. Wind speed forecasted for 24 hours using FOM and SOM is shown in Fig. 3b.

3) ARMIA Model: To determine the best fit ARIMA model, ACF and PCF are plotted as shown in Fig. 2a and Fig. 2b. It is observed from Fig. 2a, ACF is exponentially decaying which implies ARIMA(p,0,0) or AR(p) model. To determine number of AR terms to be considered, it is observed from Fig. 2b, PACF is significant till 3 lags only. Hence it is AR(3) or ARIMA(3,0,0) model. In this paper a lower and higher model of AR(3) have also been considered i.e AR(2) and AR(4). The forecasted wind speeds for AR(2), AR(3) and AR(4) are shown in Fig. 3c.

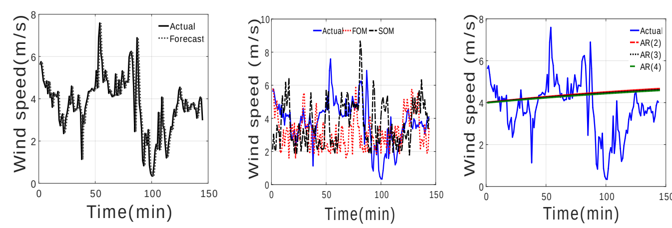

(a) Persistence (b) Markov (c) ARMA

Fig. 3: Forecast models

The mean speed obtained for the actual wind speed and for different forecast model are plotted in Fig. 4. It is observed from Fig. 4, mean wind speed obtained for persistence model is 3.77 m/s which is very close to actual wind speed 3.76 m/s, while mean speed for SOM is 3.69 m/s, slightly lower than actual wind speed. The mean wind speed for AR(2), AR(3) and AR(4) models are 4.37, 4.34 and 4.31 m/s, which are higher than the actual wind speed.

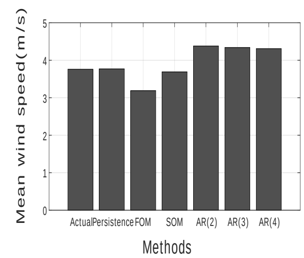

Fig. 4: Mean wind speed for different forecast models

The validation of the models is done by evaluating MAE and RMSE, it is observed from Fig. 5, RMSE is usually higher than MAE for persistence and for all AR models. It is also observed from Fig. 5, persistence forecast model performance is better than AR forecast model.

From Fig. 5, it is observed MAE and RMSE are equal for FOM and SOM. It is also observed from Fig. 3b, SOM gives better error statistics than FOM. Henceforth we have adopted SOM for wind forecasting in this paper. The performance of SOM is found to better than AR and persistence models as shown in Fig. 5. Similar result were reported in [12], where the performance of Persistence model, second order Markov model, ARMA model and Weibull model were compared and it was reported that SOM performance is best for short term wind forecast followed by ARMA and Persistence.

It is observed from Fig. 5, MAE evaluated for AR(2), AR(3) and AR(4) are 5.9, 6.1 and 5.9 respectively while RMSE values calculated for AR(2), AR(3) and AR(4) are 6.9, 7.1 and 6.8 respectively. It is also observed from Fig. 5, AR(2) and AR(4) not only give comparable error statistics but also are better than AR(3) model. According to Parsimony principle, when the validation statistic of two different model are comparable it is preferable to use lower order model as the complexity increase with the use of higher order model [26]. Hence in this paper we have adopted simpler lower order AR(2) model for wind forecasting.

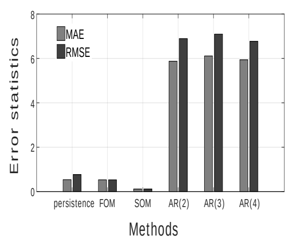

Fig. 5: Error statistics

The error forecast series for persistence, SOM and AR(2) model is obtained using (12) and normalised with respect to actual wind speed to obtain absolute normalised wind speed error series plotted on logarithm scale as shown in Fig. 6. It is observed from Fig. 6 the normalised wind speed error can be 1.9 times the actual wind speed for persistence method. For SOM, the normalised error can become 13.8 times larger than actual wind speed. For AR(2) forecasting model, normalised error can be 12.2 times larger than actual wind speed. These error are significant and will effect the real time performance of the BESS operation.

B. Impact of different forecasting method

The impact of the forecasting method accuracy on the system operation can be studied by using three different forecasted wind speed data for a day namely Naive, SOM and ARIMA(2,0,0). The dispatched interval is considered of 15 minutes. The impact of the accuracy of forecasting model on the system performance is studied by evaluating per unit values of reliability indices like EES, EENS and EENU. The impact of wind forecasting model on the rating of the BESS and on the number of charge /discharge cycle BESS undergoes

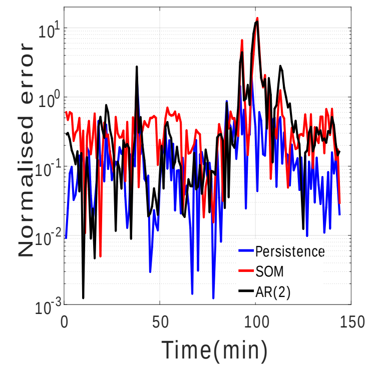

Fig. 6: Wind speed error series

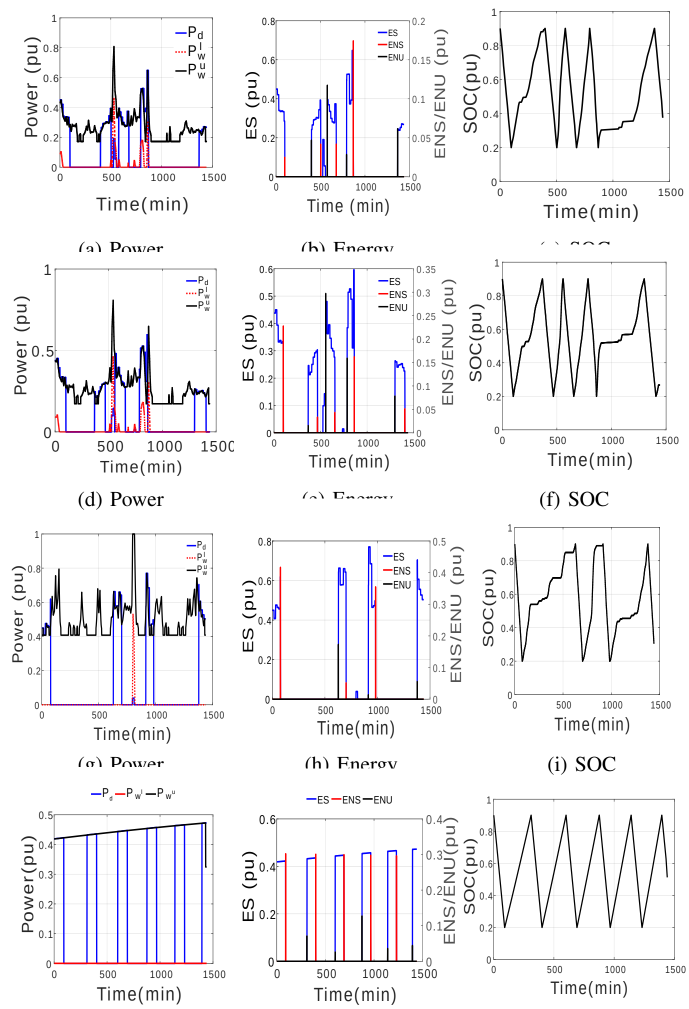

(a) Power (b) Energy (c) SOC

(d) Power (e) Energy (f) SOC

(g) Power (h) Energy (i) SOC

(j) Power (k) Energy (l) SOC

Fig. 7: The performance of min-max operating strategy for 15 min dispatch interval

in a day is also presented in this section. It is assumed at the beginning of the simulation, BESS is fully charged and SOC is maintained at maximum limit. As the BESS is fully charged it would discharge during first dispatch interval.

The performance of the system determined when the actual wind speed data is used, BESS energy capacity is assumed to be 0.3595 pu. Reliability indices ES, ENS and ENU obtained for each dispatched interval for the actual wind speed are shown in Fig. 7b. ENS is zero for all dispatched interval except for $(t = 98, 502, 677, 869)$, when the BESS at reached it lower SOC limit and can not be discharged further. Similarly ENU is zero for all dispatch interval except $(t = 399, 577, 793, 1367)$ when BESS has reached it upper SOC limit and can not be charged. ENS attains maximum value of 0.1743 pu at $t = 869$, while ENU attains maximum value 0.1173 pu at $t = 577$. From Fig. 7c it is seen that the SOC is maintained within and set limit and BESS undergoes complete charging/discharging cycle. SOC is observed to be constant (e.g t= 177-189, 205-227, 889-1048, 1089-1176) , since in these intervals the power sink or source from the BESS is very small that SOC is constant.

The wind speed forecasted using persistence model is the actual wind speed shifted by some time step, per unit dispatched power, lower and upper forecast wind power for the actual wind speed and persistence model are similar as shown in Fig. 7a and Fig. 7d. It is observed from Fig. 7d when the BESS is discharging, P_d equal to minimum value of P_w^l in the dispatch interval and P_d is zero for the intervals, if P_w^l is zero in that interval. When the BESS is charging, P_d is equal to the maximum value of P_w^u. On comparing Fig. 7e and Fig. 7d it is observed that ES plot is similar to P_d plot and ES is zero for the intervals for which P_d is zero. ENS is zero at all t except at $t = 100, 467, 654, 862, 1486$, when BESS has hit its lower SOC limit as seen from Fig. 7e and Fig. 7f. Similarly ENU is zero for all t except at $t = 367, 556, 785, 1299$, when BESS has reached its upper SOC limit. Maximum value ENS and ENU attains during the day is 0.2279 pu and 0.2973 pu respectively. SOC is maintained between the set limits $SOC^{min} - SOC^{max}$ and BESS undergoes complete charging/discharging cycles using min-max operating strategy as shown in Fig. 7f. It is also observed SOC is constant in the intervals (e.g. t=180-199, 215-238, 906-1060, 1064-1088,1100-1189)as the power source or sink by the BESS is constant, $P_d = 0$ and P_w^c is constant and negligible so during these intervals SOC remain almost constant.

The per unit values of dispatch power, lower and upper forecast power using SOM forecasted wind data are shown in Fig. 7g. It is observed from Fig. 7g, P_w^l is zero for all interval except for interval $t = 795 - 818$. On comparing Fig. 7g and Fig. 7h, it is observed ES plot is similar to P_d and ES is zero when $P_d = 0$. It is also observed from Fig. 7h and Fig. 7i, ENS is negligible for all t except at $t = 77, 702, 988$ as the SOC of BESS has reached its lower limit and can not discharge to meet the demand. ENU is zero for all t except at $t = 627, 914, 1379$ when the SOC of BESS has reached its upper limit and can not charge further, surplus wind energy has to be spilled as observed from 7h and Fig. 7i. The maximum value ENS and ENUS attains during the day is 0.4161 and 0.1731 pu respectively. SOC is maintained between the set limits $SOC^{min} - SOC^{max}$ and BESS undergoes complete charging/discharging cycles using min-max operating strategy as shown in Fig. 7i. It is also observed SOC is constant in the certain intervals as the power source or sink by the BESS is constant, $P_d = 0$ and P_w^c is constant and negligible so during these intervals SOC remain almost constant.

Dispatch power, lower and upper forecast power for the wind speed forecast using ARIMA(2,0,0) model is shown in Fig. 7j. P_w^l is zero through out the day, when BESS is charging $P_d = min(P_w^l)$ and when BESS is discharging $P_d = min(P_w^u)$ as seen in Fig. 7j. From Fig. 7j and Fig. 7k it is observed ENS and ENU are zero for all intervals except at $t = 93, 402, 693, 968, 1233$ and $t = 311, 601, 878, 1141, 1396$ respectively as the SOC of BESS has reached its set operating limits.The maximum ENS and ENU seen during the day is 0.3021 and 0.1274 pu respectively.

C. Impact of different dispatch interval

Impact of dispatched interval of wind farm on the operational performance of system is studied by considering dispatch interval of 5 min, 15 min and 1 hour. The per unit values of EES, EENS, EENU, power rating of BESS and number of BESS cycles in a day has been presented in Fig. 8 for persistence(Naive), SOM and AR(2)as shown in Fig. 3c. For the actual wind speed the EES for actual wind

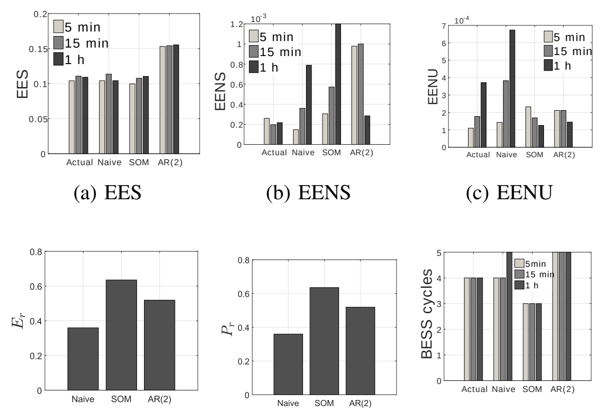

(a) EES (b) EENS (c) EENU

(d) Energy capacity (e) Power capacity (f) No. of BESS cycles

Fig. 8: The performance of min-max operating strategy using different forecast models and for different dispatch interval

increases from 0.1041 pu to 0.1107 pu when the dispatch interval increases from 5 minute to 15 minute but it reduces to 0.1092 pu when the dispatch interval is increased to an hour as shown in Fig. 8a. Since persistence model is obtain by shifting actual wind speed, EES for persistence model is expected to show similar trends as that of actual wind speed but EES for persistence model is same 0.1041 pu for 5 min and one hour dispatch interval and highest value of EES 0.1136 pu is obtained for 15 minute dispatch interval as seen in Fig. 8a. EES for the SOM increases as the dispatched interval is increased, EES is 0.0996 pu for 5 minute dispatch interval which is lower than the EES of actual wind and persistence model for the same length of interval. There is slight increase in EES from 0.1077 to 0.1107 pu when the dispatch interval is increased from 15 minute to one hour for SOM model. When the AR(2) model is used for forecasting, EES shows little improvement from 0.153 to 0.1541 pu when dispatch interval is changed from 5 minute to 15 minute as seen from Fig. 8a. It is also observed from Fig. 8a EES further improves to 0.1552 pu as the dispatch interval is increased from 15 minute to one hour for the AR(2) model.

The EENS for the actual wind is largest at 2.6×10^{-4} pu for 5 minute dispatch interval, it is higher than the EENS 2.6×10^{-4} pu for one hour dispatch interval as shown in Fig. 8b. EENS for persistence model has a different trend from the actual wind, EENS increases from 1.4×10^{-4} pu to 7.8×10^{-4} pu as the dispatch interval increases from 5 minute to one hour. Similar trend is observed for EENS obtain for SOM forecast model, EENS increases from 3.1×10^{-4} pu to 12×10^{-4} pu as the dispatch interval is increased from 5 minute to one hour as shown in Fig. 8b. For AR(2) model EENS for 5 minute and 15 minute are comparable while EENS is least for one hour dispatch interval as shown in Fig. 8b.

The EENU increases from 1.09×10^{-4} pu to 3.71×10^{-4} pu and from 1.43×10^{-4} pu to 6.73×10^{-4} pu for actual wind and persistence model when the dispatch interval is changed from 5 minute to one hour respectively as shown in Fig. 8c. For SOM forecast model, EENU shows reverse trend, it reduces from 2.32×10^{-4} pu to 1.25×10^{-4} pu as dispatch interval is increased from 5 minute to an hour as seen from Fig. 8c. It is also observed from Fig. 8c, EENU at 2.11×10^{-4} pu is comparable for 5 minute and 15 minute dispatch interval for AR(2) model but it reduces to 1.49×10^{-4} pu for one hour dispatch interval.

It is observed from Fig. 8e and Fig. 8d power and energy capacity at 0.3595 pu is lowest for persistence method and at 0.6353 pu largest for SOM. Number of BESS cycles are lowest for SOM and highest for AR(2) model as shown in Fig. 8f for 5 minute, 15 minute and one hour dispatch interval. Number of BESS cycles are same for actual wind and persistence model for 5 minute and 15 minute dispatch interval but for one hour, BESS cycles are more for persistence model as shown in Fig. 8f.

VII. Conclusion

Three different time series based forecasting method are studied and compared. The impact of the forecasting methods on the operation of the WPP with the BESS is evaluated by calculating EES, EENS and EENU. Impact of the forecasting method on the power rating of the BESS is also presented in the paper. Second order Markov model gave better statistic than Naive and ARIMA(2,0,0) but energy served is more when ARIMA(2,0,0) forecasting model is used, followed by Naive and Markov model. When SOM model is used for wind forecasting BESS undergoes least number of cycles but when AR(2) wind forecasting model is used BESS undergoes highest number of cycles. BESS energy and power rating is highest for SOM and least for Naive model.

References

[1] S. S. Soman, H. Zareipour, O. Malik, and P. Mandal, "A review of wind power and wind speed forecasting methods with different time horizons," in *North American Power Symposium 2010*. IEEE, 2010, pp. 1–8.

[2] A. M. Foley, P. G. Leahy, A. Marvuglia, and E. J. McKeogh, "Current methods and advances in forecasting of wind power generation," *Renewable Energy*, vol. 37, no. 1, pp. 1–8, 2012.

[3] N. R. Ullah, K. Bhattacharya, and T. Thiringer, "Wind farms as reactive power ancillary service providerstechnical and economic issues," *IEEE Transactions on Energy Conversion*, vol. 24, no. 3, pp. 661–672, 2009.

[4] R. G. Kavasseri and K. Seetharaman, "Day ahead wind speed forecasting using f-arima models," *Renewable Energy*, vol. 34, no. 5, pp. 1388–1393, 2009.

[5] A. Tesfaye, J. Zhang, D. Zheng, and D. Shiferaw, "Short-term wind power forecasting using artificial neural networks for resource scheduling in microgrids," *International Journal of Science and Engineering Applications (IJSEA)*, vol. 5, no. 3, 2016.

[6] M. Lange and U. Focken, "New developments in wind energy forecasting," in *2008 IEEE power and energy society general meeting-conversion and delivery of electrical energy in the 21st century*. IEEE, 2008, pp. 1–8.

[7] A. Bizrah and M. AlMuhaini, "Modeling wind speed using probability distribution function, markov and arma models," in *2015 IEEE Power & Energy Society General Meeting*. IEEE, 2015, pp. 1–5.

[8] A. Carpinone, M. Giorgio, R. Langella, and A. Testa, "Markov chain modeling for very short term wind power forecasting," *Electric Power Systems Research*, vol. 122, pp. 152–158, 2015.

[9] H. Madsen, P. Pinson, G. Kariniotakis, H. A. Nielsen, and T. S. Nielsen, "Standardizing the performance evaluation of short-term wind power prediction models," *Wind engineering*, vol. 29, no. 6, pp. 475–489, 2005.

[10] H. Bludszuweit, J. A. Domínguez-Navarro, and A. Llombart, "Statistical analysis of wind power forecast error," *IEEE Transactions on Power Systems*, vol. 23, no. 3, pp. 983–991, 2008.

[11] L. Kamal and Y. Z. Jafri, "Time series models to simulate and forecast hourly averaged wind speed in quetta, pakistan," *Solar Energy*, vol. 61, no. 1, pp. 23–32, 1997.

[12] T. R. Ayodele, R. Olarewaju, and J. L. Munda, "Comparison of different wind speed prediction models for wind power application," in *2019 Southern African Universities Power Engineering Conference/Robotics and Mechatronics/Pattern Recognition Association of South Africa (SAUPEC/RobMech/PRASA)*. IEEE, 2019, pp. 223–228.

[13] P. J. Brockwell, R. A. Davis, and M. V. Calder, *Introduction to time series and forecasting*. Springer, 2002, vol. 2.

[14] I. N. Moghaddam, B. H. Chowdhury, and S. Mohajeryami, "Predictive operation and optimal sizing of battery energy storage with high wind energy penetration," *IEEE Transactions on Industrial Electronics*, vol. 65, no. 8, pp. 6686–6695, 2018.

[15] X. Ke, N. Lu, and C. Jin, "Control and size energy storage systems for managing energy imbalance of variable generation resources," *IEEE Transactions on Sustainable Energy*, vol. 6, no. 1, pp. 70–78, 2014.

[16] Q. Li, S. S. Choi, Y. Yuan, and D. Yao, "On the determination of battery energy storage capacity and short-term power dispatch of a wind farm," *IEEE Transactions on Sustainable Energy*, vol. 2, no. 2, pp. 148–158, 2011.

[17] C. L. Nguyen, T. W. Chun, and H. H. Lee, "Determination of the optimal battery capacity based on a life time cost function in wind farm," in *2013 IEEE Energy Conversion Congress and Exposition*. IEEE, 2013, pp. 51–58.

[18] T. S. Nielsen, A. Joensen, H. Madsen, L. Landberg, and G. Giebel, "A new reference for wind power forecasting," *Wind Energy: An International Journal for Progress and Applications in Wind Power Conversion Technology*, vol. 1, no. 1, pp. 29–34, 1998.

[19] G. E. Box, G. M. Jenkins, G. C. Reinsel, and G. M. Ljung, *Time series analysis: forecasting and control*. John Wiley & Sons, 2015.

[20] A. Shamshad, M. Bawadi, W. W. Hussin, T. Majid, and S. Sanusi, "First and second order markov chain models for synthetic generation of wind speed time series," *Energy*, vol. 30, no. 5, pp. 693–708, 2005.

[21] A. D. Sahin and Z. Sen, "First-order markov chain approach to wind speed modelling," *Journal of Wind Engineering and Industrial Aerodynamics*, vol. 89, no. 3-4, pp. 263–269, 2001.

[22] H. Nfaoui, H. Essiarab, and A. Sayigh, "A stochastic markov chain model for simulating wind speed time series at tangiers, morocco," *Renewable Energy*, vol. 29, no. 8, pp. 1407–1418, 2004.

[23] K. Brokish and J. Kirtley, "Pitfalls of modeling wind power using markov chains," in *2009 IEEE/PES Power Systems Conference and Exposition*. IEEE, 2009, pp. 1–6.

[24] S. M. Verma, V. Reddy, K. Verma, and R. Kumar, "Markov models based short term forecasting of wind speed for estimating day ahead wind power," in *2018 International Conference on Power, Energy, Control and Transmission Systems (ICPECTS)*. IEEE, 2018, pp. 31–35.

[25] C. W. Potter and M. Negnevitsky, "Very short term wind forecasting for tasmanian power generation," *IEEE Transactions on Power Systems*, vol. 21, no. 2, pp. 965–972, 2006.

[26] B. R. Bhat, *Stochastic models: analysis and applications*. New Age International, 2004.